J Biomol NMR (2015) 61:151–160
DOI 10.1007/s10858-015-9902-2

ARTICLE

Perspectives for sensitivity enhancement in proton-detected solid-state NMR of highly deuterated proteins by preserving water magnetization

Veniamin Chevelkov · ShengQi Xiang · Karin Giller · Stefan Becker · Adam Lange · Bernd Reif

Received: 11 September 2014 / Accepted: 19 January 2015 / Published online: 30 January 2015

Abstract In this work, we show how the water flip-back approach that is widely employed in solution-state NMR can be adapted to proton-detected MAS solid-state NMR of highly deuterated proteins. The scheme allows to enhance the sensitivity of the experiment by decreasing the recovery time of the proton longitudinal magnetization. The method relies on polarization transfer from non-saturated water to the protein during the inter-scan delay.

Keywords Magic angle spinning (MAS) solid-state NMR · Perdeuteration · Sensitivity enchancement · Protein water interaction

Electronic supplementary material The online version of this article (doi:10.1007/s10858-015-9902-2) contains supplementary material, which is available to authorized users.

V. Chevelkov · S. Xiang · K. Giller · S. Becker · A. Lange
Max-Planck-Institut für biophysikalische Chemie (MPI-bpc), Am Fassberg 11, 37077 Goettingen, Germany

V. Chevelkov (✉) · A. Lange
Leibnizinstitut für Molekulare Pharmakologie (FMP), Robert-Rössle-Str. 10, 13125 Berlin, Germany
e-mail: shevelkov@fmp-berlin.de

A. Lange
Institut für Biologie, Humboldt Universität zu Berlin, Invalidenstr 110, 10115 Berlin, Germany

B. Reif
Munich Center for Integrated Protein Science (CIPS-M), Department Chemie, Technische Universität München (TUM), Lichtenbergstr. 4, 85747 Garching, Germany

B. Reif
Helmholtz-Zentrum München (HMGU), Deutsches Forschungszentrum für Gesundheit und Umwelt (HMGU), Ingolstädter Landstr. 1, 85764 Neuherberg, Germany

Introduction

Solid-state NMR (ssNMR) spectroscopy of rotating solids progressed rapidly during the last decade as a unique and powerful tool to study the atomic-resolution structure (Helmus et al. 2008; Loquet et al. 2012; Wasmer et al. 2008) and dynamics (Chevelkov et al. 2009; Schanda et al. 2010) of biological macromolecules. Application of magic angle spinning (MAS) ssNMR is limited due to its inherently low sensitivity. A number of developments have been made in order to overcome this obstacle. One promising approach in biomolecular ssNMR is to employ proton detection and to make use of the high gyromagnetic ratio of protons. These experiments became feasible by employing deuterated samples and/or high frequency sample rotation (Chevelkov et al. 2003; Paulson et al. 2003; Zhou et al. 2007a). Proton spin dilution can be employed to facilitate the study of protein structure and dynamics (Chevelkov et al. 2009; Huber et al. 2011; Knight et al. 2011; Linser et al. 2011; Schanda et al. 2010; Zhou et al. 2007b).

In most ssNMR experiments, more than 90 % of the measurement time is used for longitudinal spin relaxation. Thus, data collection can be accelerated if the recovery time of the spin system is reduced and spins reach faster their thermal equilibrium within a shorter inter-scan delay. This can be achieved, for example, by doping the sample with complexed paramagnetic ions (Ganapathy et al. 1981) which directly reduces the longitudinal relaxation time. For biological ssNMR, paramagnetic relaxation enhancement has been introduced recently by Ishii and co-workers (Wickramasinghe et al. 2009). In protonated samples, this method requires rapid magic angle sample spinning, low proton power decoupling, robustness of the probe with respect to short repetition delays, and sample stability to withstand significant heating as a consequence of radio

frequency (RF) irradiation during decoupling. The doping agent must not tumble freely in solution, but can be bound directly to the protein, attached via a tag (Nadaud et al. 2010), or to the lipid membrane (Yamamoto et al. 2010). Use of perdeuterated proteins allows to avoid the detrimental consequences of high-power RF irradiation, yielding high spectral resolution while preserving sample integrity (Linser et al. 2007).

Recently, it has been shown that the longitudinal magnetization recovery time of selected ^{13}C resonances can be reduced by selective excitation of a specific carbon spectral region (Giffard et al. 2009; Lopez et al. 2009). Spin magnetization exchange between selectively excited ^{13}C atoms and the remaining carbon pool significantly reduces longitudinal magnetization recovery time and allows speeding up measurements observing only resonances within a limited ^{13}C bandwidth. Band selective longitudinal relaxation enhancement has been demonstrated for the tripeptide MLF (Lopez et al. 2009), for histidine and the two proteins MerP and YajG (Giffard et al. 2009).

In solid-state NMR, a substantial fraction of the proton magnetization is not transferred after cross-polarization (CP) from ^{1}H to a low-γ nucleus (mostly ^{15}N and ^{13}C). Recycling of this magnetization has a great potential to improve sensitivity, especially in protein ssNMR, because the water pool contains the majority of the ^{1}H polarization, which is not actively used. Experiments which avoid the complete destruction of ^{1}H magnetization to enhance longitudinal relaxation are well known in ssNMR (Lupulescu and Frydman 2011; Saito et al. 2011; Tegenfeldt and Haeberlen 1979). In these experiments, the residual ^{1}H magnetization is flipped back along the axis of the static magnetic field after H–C/N CP. This flip-back pulse facilitates spin recovery to its equilibrium state after detection of carbon or nitrogen signal. A limitation of these approaches is that proton decoupling must be employed in order to obtain high-resolution ^{13}C and ^{15}N spectra, which reduces the remaining proton polarization and decreases the recovery efficiency of the proton magnetization of interest. As a requirement, the decoupling pulse sequence is supposed to destroy the residual proton magnetization as little as possible, resulting in a compromise between heteronuclear decoupling performance and loss of the residual ^{1}H magnetization during decoupling. Very often these approaches suffer from low resolution, as only sub-optimal heteronuclear decoupling schemes can be employed.

Highly deuterated proteins do not require high-power proton decoupling to obtain ultrahigh resolution spectra (Chevelkov et al. 2006). This makes deuterated proteins ideally suited to preserve and reuse the residual ^{1}H polarization to speed up the recovery of proton longitudinal magnetization. A proton flip-back approach was successfully applied in carbon-detected experiments on highly deuterated PrgI needles (Chevelkov et al. 2013). Samples of this kind do not require proton–carbon heteronuclear decoupling, thus, the residual proton magnetization could be efficiently preserved along the external magnetic field during ^{13}C detection. Overall, a gain of sensitivity of a factor of 1.6 was obtained. However, carbon detection in deuterated proteins is in general not efficient. Therefore, this technique has certain practical limitations. In deuterated spin systems, proton detection is possible and very often required to achieve high sensitivity. The experimental design principles can be adapted from modern solution-state NMR spectroscopy. In solution-state NMR, a minimization of the proton longitudinal magnetization recovery time can be achieved by the transfer of magnetization from the not saturated water (Grzesiek and Bax 1993; Mori et al. 1995; Stonehouse et al. 1994) and/or protein protons which are not observable in the given experiment (Atreya and Szyperski 2004; Pervushin et al. 2002). Schanda and Brutscher (Schanda and Brutscher 2005) could show that a two-dimensional HMQC spectrum can be acquired within 5 s by utilizing proton longitudinal relaxation enhancement, featuring a small number of RF pulses and Ernst angle excitation (Ernst et al. 1987). These schemes are not directly transferable to solid-state MAS NMR, because solid-state NMR pulse sequences employ mostly cross-polarization instead of INEPT for inter nuclear magnetization transfer.

In this work, we present a new pulse scheme to enhance the sensitivity of proton-detected MAS solid-state NMR experiments, utilizing magnetization transfer from the non-saturated water and the residual protons of the protein to amide protons during the inter-scan delay. 2D H_iN_i and 3D $H_iCO_{i-1}CA_{i-1}$ correlation experiments were recorded to demonstrate the approach. A proton flip-back (FB) pulse is used to preserve the residual ^{1}H magnetization along the external magnetic field. The experiments are demonstrated using an insoluble, non-crystalline biological assembly, the Salmonella typhimurium type III secretion system (T3SS) needle. Perdeuterated and uniformly ^{13}C- and ^{15}N-labeled PrgI subunit was subsequently re-protonated in a buffer containing D_2O and H_2O at a ratio of 4:1. Recently, Akbey et al. (2010) have shown that the optimal proton density for the α-SH3 domain is 30–40 %. Because of considerably lower resolution demonstrated by the PrgI needles, we use lower concentration of exchangeable protons to maintain single residue resolution in 2D HN spectra. Proton and nitrogen average line widths in 2D heteronuclear correlation (HETCOR) spectra obtained for this sample at moderate sample spinning rates without proton dipolar decoupling are 47 Hz and 19 Hz, respectively.

Materials and methods

Expression, purification, and polymerization of perdeuterated ^{15}N- and ^{13}C-labelled wild-type PrgI protein were performed as described before (Chevelkov et al. 2013; Loquet et al. 2011, 2012). A low degree of protonation in the samples was achieved by employing the approach described earlier by Reif and co-workers (Chevelkov et al. 2006). The sample was prepared using a buffer containing 20 % H_2O. Approximately 3.5 mg of protein was packed into a 2.5 mm rotor. First, the rotor was spun at 25 kHz during $\sim$20 h, after that the excess of buffer was removed to minimize water artifacts during detection.

Solid-state NMR experiments were conducted using a 600 MHz (^{1}H Larmor frequency) spectrometer (Bruker Biospin, Germany) equipped with a (^{1}H, X, Y) triple-resonance 2.5 mm probe. The sample was spun at 25 kHz. The effective sample temperature was 10 $\pm$ 2 °C as measured by the temperature-dependent water proton resonance relative to an internal DSS reference (Boeckmann et al. 2009). Chemical shift referencing was achieved using the internal DSS reference.

The presented experiments are based on proton detection and the constant time approach, as introduced by Zilm and co-workers (Paulson et al. 2003) for suppression of the residual water proton signal. Magnetization transfers between different nuclei were achieved by recoupling of hetero- or homonuclear dipolar interactions. For this purpose, common recoupling techniques such as cross-polarization (CP) (Pines et al. 1972), SPECIFIC-CP (Baldus et al. 1998), HORROR, or DREAM (Nielsen et al. 1994; Verel et al. 2001) were employed. Details concerning the employed RF field strengths and shaped pulses are listed in Table S1 (Supporting Information) for each experiment. For homonuclear double-quantum transfers, a continuous ^{13}C RF irradiation was applied in the middle of the CA band, while the CO magnetization was aligned by the trim pulse along the effective RF field defined by the chemical shift offset and the applied RF field. No high-power proton decoupling was applied during the chemical shift evolution periods and the polarization transfer steps between low γ nuclei. Gaussian pulse cascades (Emsley and Bodenhausen 1990) were used for band-selective 180° pulses on CO and CA. When required, suppression of the remaining solvent proton magnetization was achieved by a proton pulse train comprising high- and low-power pulses (Chevelkov et al. 2014; Zhou and Rienstra 2008). Heteronuclear *J* decoupling was applied during all chemical shift evolution periods. Homonuclear CO-CA scalar couplings were removed only during indirect CO chemical shift evolution periods. All NMR spectra were analyzed using CCPNMR (Vranken et al. 2005). More experimental details are provided in the Supporting Information.

Results and discussions

Sensitivity enhancement employing water flip-back pulse

According to the experimental requirements and the limitations described in the introduction, the designed pulse sequence should possess a number of specific features. A basic requirement is that high-power multi-pulse decoupling schemes such as TPPM which destroy the residual proton magnetization cannot be employed. A potential solution of this problem is the use of highly deuterated samples to obtain high resolution spectra. For those samples, 180° pulses are sufficient to refocus heteronuclear scalar couplings during the ^{15}N evolution period. Even in such systems selective proton pulses are not as efficient as in solution-state NMR where they are utilized to selectively preserve proton magnetization of water and specific regions of the protein. This advocates the use of hard pulses. In general, magnetization transfers between ^{1}H and ^{15}N or ^{13}C are more efficient using CP in comparison to INEPT. These pre-conditions set the stage for the design of pulse sequences which re-use the preserved magnetization of water of and residual protons of a protein.

Figure 1a represents the new proton-detected ^{1}H,^{15}N 2D HETCOR pulse scheme employing a proton flip-back pulse to decrease the ^{1}H longitudinal magnetization recovery time. The experiment is based on a 2D heteronuclear correlation experiment described earlier (Chevelkov et al. 2006; Paulson et al. 2003) which is represented in Fig. 1b. Modifications in the new scheme are given in red color. In the experiment, an initial cross-polarization element is followed by a hard 90° proton pulse to flip the residual proton magnetization along the –Z-axis. The proton 180° hard pulse, applied in the middle of the indirect evolution period to achieve ^{1}H-^{15}N scalar decoupling, returns the magnetization back to the +Z-axis. Thus, aligned along the external magnetic field the remaining proton magnetization of water and the protein is preserved. For detection, nitrogen magnetization is back-transferred by a ramped CP step to protons, while the remaining proton polarization is preserved along the +Z-axis. This can be achieved by a proton spin-lock preceding or following the CP transfer. This spin-lock pulse has an inverted phase, but the same duration as the RF field applied to the ^{1}H channel during CP. For proton–nitrogen CP, the nitrogen RF field was ramped from 70 to 100 % with an average value of 35 kHz, while the proton RF field strength was kept constant at 60 kHz. During the CP "back" transfer from nitrogen to protons, the nitrogen RF field was ramped down from 100 to 70 %, employing the same RF field amplitudes as for the first CP. The CP contact times were set to 0.85 and 0.41 ms for the proton–nitrogen and the nitrogen–proton transfer,

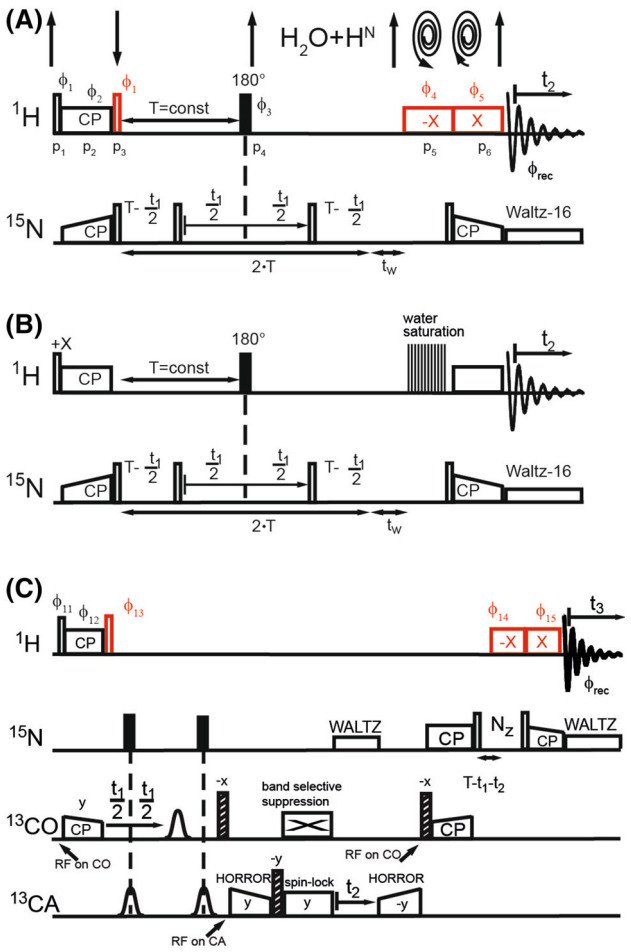

Fig. 1 **a** Flip-back HETCOR pulse sequence to record proton-detected 2D ^{1}H,^{15}N correlation spectra for a highly deuterated protein sample in the solid state. The *upper row* schematically represents a trajectory of the residual proton magnetization during the experiment. Pulse sequence elements highlighted in *red color* represent modifications of a standard 2D HN correlation, plotted in the *panel* below. The phase cycle is $\phi_1 = \{x,-x\}$, $\phi_2 = 32 \times \{-y\},32 \times \{y\}$, $\phi_3 = \{x\}$, $\phi_4 = 2\times\{-x,-x,x,x\}$, $2 \times \{x,x,-x,-x\}$, $\phi_5 = -\phi_4$, $\phi_{rec} = \{x,-x,-x,x\ -x,x,x,-x\ -x,x,x,-x\ x,-x,-x,x\ -x,x,x,-x\ x,-x,-x,x\ -x,x,x,-x\ x,-x,-x,x\ -x,x,x,-x\ x,-x,-x,x\ -x,x,x,-x\ x,-x,-x,x\ -x,x,x,-x\ x,-x,-x,x\}$. **b** Regular HETCOR pulse sequence without a flip-back pulse. **c** 3D proton-detected (H)COCA(CON)H pulse sequence to obtain inter-residual H_i^N,CA_{i-1},CO_{i-1} correlation spectra for sequential backbone assignment. Pulse sequence elements highlighted in *red color* represent modifications of the previously described 3D proton-detected (H)COCA(CON)H pulse sequence (Figure S1B). In all pulse schemes, *open, filled*, and *hatched bars* represent 90°, 180°, and trim pulses, respectively. *Bell shapes* correspond to band-selective 180° pulses (Emsley and Bodenhausen 1990). The phase cycle is $\phi_{11} = 4\times\{y\}$, $4 \times \{-y\}$, $\phi_{12} = \{x,-x\}$, $\phi_{13} = -\phi_{11}$, $\phi_{14} = 16 \times \{-x\}$, $16 \times \{x\}$, $\phi_{15} = -\phi_{14}$, $\phi_{rec} = \{x,-x,-x,x\ -x,x,x,-x\ -x,x,x,-x\ x,-x,-x,x\ -x,x,x,-x\ x,-x,-x,x\ -x,x,x,-x\ x,-x,-x,x\ -x,x,x,-x\ x,-x,-x,x\ -x,x,x,-x\ x,-x,-x,x\ -x,x,x,-x\ x,-x,-x,x\ -x,x,x,-x\ x,-x,-x,x\}$. The experiments were carried out using a spectrometer operating at a proton Larmor frequency of 600 MHz. The MAS frequency was set to 25 kHz. The effective sample temperature was adjusted to 10 °C

respectively. During proton detection, heteronuclear scalar decoupling is achieved by application of WALTZ-16 on the ^{15}N channel. The water dephasing delay t_w and the constant time period T were set to optimize water suppression and were in a range of 2–10 ms and 40–50 ms, respectively. In general, water suppression and sensitivity enhancement depend on the duration and the strength of the proton pulses p_1, p_2, p_3, p_4, p_5, and p_6 (Fig. 1a), which might require more careful optimization in comparison with a regular HETCOR experiment. In practice, we found that the duration of the pulses p_3, p_4, and p_5 has pronounced effects on solvent suppression. The flip angle of these pulses has to be calibrated with an accuracy of ca. 2°. Furthermore, the duration of p_5 might differ from the duration of p_6 to achieve the best sensitivity enhancement. We ascribe this to instability of the employed hardware. The optimal duration of the CP contact time in FB experiments was the same as in regular experiments.

Figure 1c shows a (H)COCA(CON)H pulse scheme employing a proton flip-back pulse to enhance the sensitivity of a $H_iCO_{i-1}CA_{i-1}$ correlation experiment introduced earlier for backbone assignment of highly deuterated proteins (Chevelkov et al. 2014) (see Figure S1, B). Some minor modifications (highlighted in red color) allow recycling of the residual proton magnetization. The experimental design follows the principles introduced for FB-HN 2D correlation experiments.

In the FB experiment, the longitudinal magnetization of the amide protons recovers considerably faster during the recovery period τ_{rec} as compared to the longitudinal magnetization in a standard experiment (Fig. 2 for the bulk 1D H^N signal). Figure 2a shows the first 1D from the (H)NH FB-HETCOR and the regular experiment recorded for different recovery times τ_{rec} as indicated in the figure. Figure 2c shows the first 1D from the (H)COCA(CON)H proton flip-back and the regular experiment recorded for different recovery times τ_{rec} as indicated in the figure. Clearly, the sensitivity of the spectra employing the new scheme is improved. The benefits in the (H)COCA(CON)H experiment are more pronounced.

Figures 2b, d illustrate the achievable sensitivity per unit time of the flip-back and the regular HETCOR experiments employing different inter-scan delays τ_{rec}. The measurements for the panel B and D have been conducted using HNH and HCOCACONH magnetization transfer schemes, respectively. The sensitivity is determined as the integral amide proton intensity (in the region from 7 to 11 ppm) divided by $(T_{scan})^{1/2}$. T_{scan} refers to the overall duration of a single experimental scan, comprising the acquisition time, the recycle delay, and the length of the pulse sequence. In our case, T_{scan} was set to $T_{scan} = \tau_{rec} + 0.115$ s. The FB pulse schemes yield their best

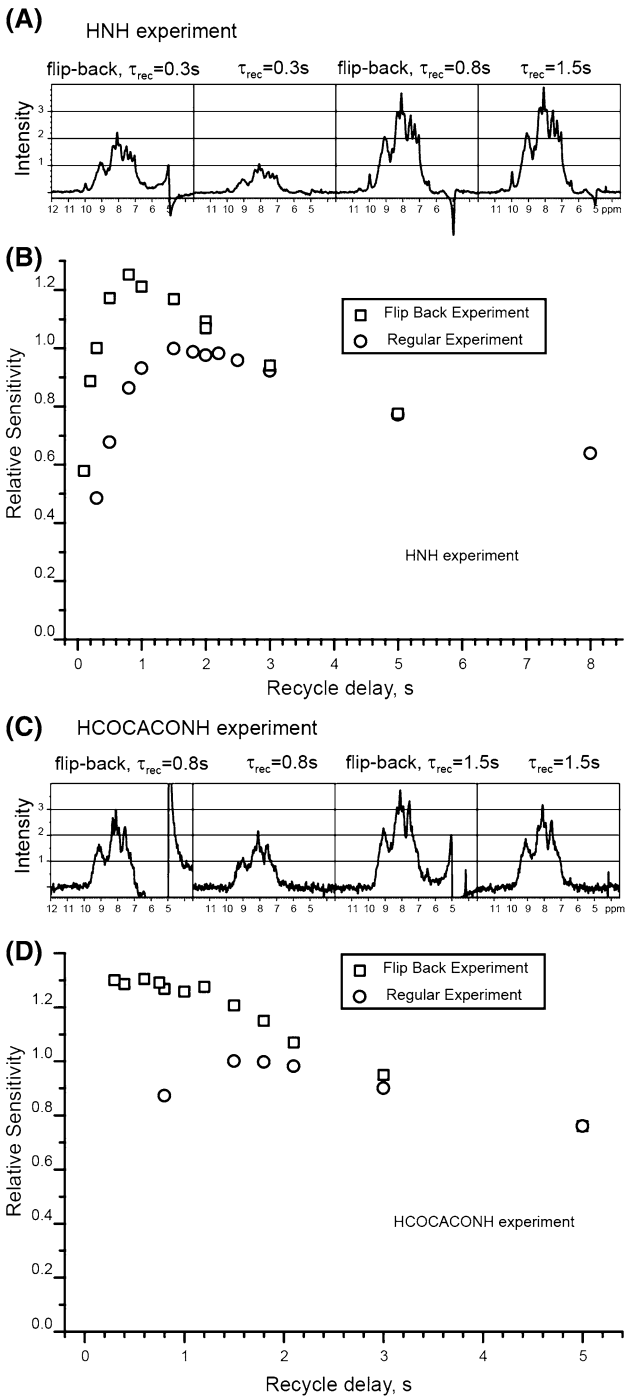

Fig. 2 **a** 1D FB-HETCOR and regular HETCOR spectra (first FID) recorded with the HNH scheme, using different recycle delays. **b** Relative sensitivity of the HNH experiment using water flip-back (*open squares*) and the regular experiment (*open circles*) as a function of the recycle delay. **c** 1D FB-HETCOR and regular HETCOR spectra (first FID) recorded with the HCOCACONH scheme, using different recycle delays. **d** Relative sensitivity of the HCOCACONH experiment using water flip-back (*open squares*) and the regular experiment (*open circles*) as a function of the recycle delay. The data in **a** and **b** were acquired with 64 scans, while the data in **c** and **d** were recorded with 128 scans

performance by using inter-scan delays of 0.8 s for both the HNH and HCOCACONH schemes. A detailed study of the amide proton magnetization' recovery dynamics is given below.

The amount of preserved proton polarization is a very important determinant of the efficiency of the flip-back sequence. The remaining proton magnetization after the different elements of the flip-back HETCOR experiment (Fig. 1a) is presented in Figure S2 (Supporting Information). About 40 and 30 % of the initial amide magnetization is preserved after the first CP step and after the entire sequence, respectively. The bulk water signal amounts to about 75 % of the initial value after the first CP step and does not change significantly during the pulse sequence. In our sample, the residual amount of protons on aliphatic side chains is too low to contribute significantly to the observed effect.

Furthermore, we investigated the performance of the FB approach for 2D and 3D experiments. Figure 3 demonstrates the sensitivity enhancement of the amide backbone signals as a function of residue obtained by FB-HETCOR (Fig. 1a) in comparison with standard HETCOR experiments (Fig. 1b, Fig. S1A). Black squares indicate enhancement values obtained for a standard HETCOR experiment employing a proton 180° hard pulse in the middle of the ^{15}N evolution period to remove the HN scalar

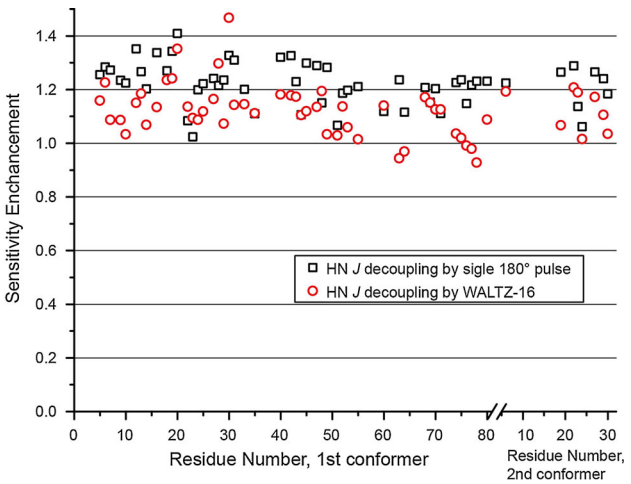

Fig. 3 Sensitivity enhancement of amide backbone resonances as a function of residue in PrgI, obtained by the FB-HETCOR scheme in comparison with the standard HETCOR experiment. *Black squares* and *red circles* indicate enhancement values compared to standard reference experiments, employing a 180° ^{1}H pulse or WALTZ-16 heteronuclear scalar decoupling. All experiments were recorded employing the same experimental parameters. In particular, all spectra were recorded with 64 scans for each increment. The recovery time τ_{rec} for subsequent experiments was chosen to obtain maximum sensitivity and was equal to 0.8 and 2.2 s for the FB-HETCOR and the regular experiments, respectively

coupling (Fig. 1b). Red circles indicate enhancement values obtained for a standard HETCOR experiment employing WALTZ-16 (Shaka et al. 1983) applied on the proton channel during the ^{15}N evolution period to remove the HN scalar coupling (Figure S1A). WALTZ-16 yields ca. 10 % more narrow nitrogen resonances in comparison with decoupling using a single 180° hard pulse (Chevelkov et al. 2014). Therefore, the observed sensitivity enhancement is smaller if the experimental outcome is compared with a reference experiment in which WALTZ-16 is employed for decoupling. All three spectra were recorded using the same parameters: for each experiment, 64 scans are accumulated. The inter-scan delay τ_{rec} for each experiment was chosen to obtain maximum sensitivity and was equal to 0.8 and 2.2 s in case of the proton flip-back and the regular experiments, respectively. The acquisition time in the direct and the indirect dimensions was set to 30.1 and 38.4 ms, respectively. The measurement time for the FB and the regular experiment was 2.05 and 5.3 h, respectively. The relative sensitivity of an individual peak S_t is given by the expression:

$$S_t = \frac{\text{Int}}{\sqrt{N_{sc} \cdot T_{exp}}} \quad (1)$$

where Int refers to amplitude of the individual amide cross-peak. T_{exp} and N_{sc} are the overall experimental time and the number of scans, respectively. The new approach yields quite uniform signal enhancements along the backbone with an average value of 1.22 and 1.11 for the experiment employing a 180° ^{1}H pulse or WALTZ-16 for decoupling. These improvements yield a gain in measurement time by a factor 1.5 or 1.23 for the respective experiment.

Under the given experimental conditions, application of a multi-pulse decoupling sequence on the ^{1}H channel during ^{15}N evolution is preferable, since it yields ca. 10 % more narrow ^{15}N lines in comparison to an experiment in which a single 180° hard proton pulse in the middle of the ^{15}N evolution is employed for decoupling (Chevelkov et al. 2014). Thus, even though the 1D proton flip-back experiment based on the HNH magnetization transfer shows an attractive enhancement in sensitivity, the sensitivity gain for the 2D HN experiments employing proton flip-back approach is smaller, because of signal broadening due to imperfect scalar decoupling in the indirect dimension. This effect is well demonstrated in the Fig. 3 which compares the FB-HETCOR and the regular HETCOR experiment, employing different HN scalar decoupling schemes. Thus, the flip-back experiment demonstrates a compromise between heteronuclear decoupling performance and sensitivity enhancement. This effect was discussed earlier for other type of FB experiments (Lupulescu and Frydman 2011; Saito et al. 2011; Tegenfeldt and Haeberlen 1979). Employing a proton concentration of 30–40 % is optimal from a sensitivity point of view (Akbey et al. 2010). But at higher reprotonation level, ^{15}N lines are broader because of increased nitrogen– and proton– proton dipolar couplings. Under these conditions, ^{15}N lines narrowing achieved by a multi-pulse decoupling sequence applied on the ^{1}H channel is expected to be more efficient and would result in lower gain of the FB approach. Thus, developing a decoupling scheme which does not destroy the remaining proton magnetization during the ^{15}N evolution is a vital requirement to benefit from the FB approach on samples that contain a higher concentration of exchangeable protons. At the current deuteration level, WALTZ-16 can reduce the ^{15}N lines width from 18.8 to 16.3 Hz, but it requires long acquisition time to observe these mild benefits and might be not always practically gainful. For 3D and 4D experiments, the ^{15}N evolution time is relatively short and strongly limits the observable line width. Under these conditions, the difference in performance of WALTZ-16 and a single ^{1}H 180° pulse for decoupling is less pronounced, and the proton flip-back approach seems to become more attractive.

In the 3D H_i^N,CA $_{i-1}$,CO$_{i-1}$ correlation based on the FB-(H)COCA(CON)H pulse scheme (Fig. 1c), evolution of the ^{15}N dimension is omitted. CO and CA nuclei do not have scalar interactions to protons and have very small dipolar couplings to protons. Therefore, the application of a multi-pulse decoupling scheme on the proton channel is not required. This makes the (H)COCA(CON)H highly suited for the flip-back approach.

Omission of water saturation results in a larger water artifact signal during proton detection in comparison to schemes using proton saturation pulses (Zhou and Rienstra 2008). This is clearly illustrated by Fig. 2a, c. Our experiments show that the achievable solvent suppression at 64 scans is sufficient to record artifact-free 2D HN correlation. The 3D (H)COCA(CON)H experiment has approximately a 10 times smaller protein signal in comparison with the 2D (H)NH experiment; thus, large number of scans is required to suppress the water artifact signal. At the same time, using more than 32 scans results in unacceptably long measurements. In order to carry out this 3D experiment with good sensitivity and resolution in a reasonable time frame with minimal water artifacts, we adopted a non-uniform sampling scheme that covered 25 % of the full sampling. This way, the number of scans could be increased to 64 to improve solvent suppression. Acquisition times were 5.3, 15.7, and 28.1 ms for the CA, CO, and H dimensions, respectively. The interscan delay was set to 0.72 s, which yields a sensitivity enhancement of a factor of 1.3 in 1D version of this experiment. The overall measurement time amounted to 17.2 h. By contrast, the regular 3D (H)COCA(CON)H experiment without water flip-back was recorded within 42 h using 16 scans (Chevelkov et al.

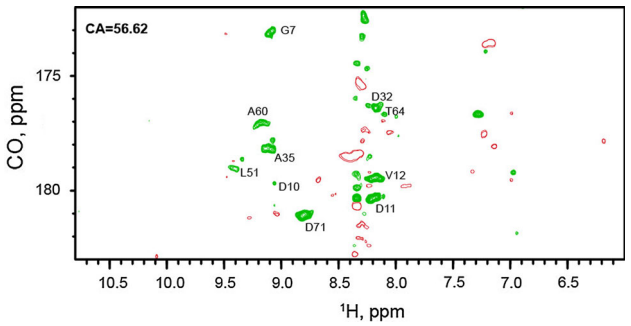

Fig. 4 2D H_iCO_{i-1} plane from the (H)COCA(CON)H 3D experiment at the CA chemical shift of 56.62 ppm. A strong water artifact is observed between 8.2 and 8.4 ppm

2014). The sparsely sampled dataset was reconstructed using the MDDnmr software (Orekhov et al. 2003). The data were further processed with NMRpipe (Delaglio et al. 1995). Figure 4 represents a 2D H_i-CO_{i-1} plane at a CA chemical shift value of 56.69 ppm. We find that the water artifact signal could be minimized using this procedure. All except 8 H_i^N,CA_{i-1},CO_{i-1} correlations are observed. The missing correlations were strongly affected by the water artifact. We expect that use of pulse field gradients will allow to improve the spectral quality in the future (Chevelkov et al. 2003).

Water and amide proton interactions

The obtained sensitivity enhancement is based on magnetization transfer from water and hydroxyl protons of the protein to the amide protons. In order to test the hypothesis whether ^1H,^1H dipolar recoupling yields an increase in sensitivity of the experiment, we applied dipolar recoupling during the recovery period. However, application of DREAM (Verel et al. 2001) or RFDR (Bennett et al. 1998) during the recovery time τ_{rec} resulted in lower sensitivity than in the regular experiment (data not shown). This behavior could be due to a fast water and amide proton magnetization decay during recoupling, which might be caused by residual dipolar proton–proton interactions, RF field inhomogeneity, and relaxation.

To investigate in detail the kinetics of the relaxation enhancement, we examined the spin diffusion dynamics from water and residual protons to the amide protons of the protein. We followed the approach introduced earlier by Chevelkov et al. (2005), which is based on selective suppression of amide protons and subsequent transfer of the preserved water magnetization to the amide protons. In the experiment, we employed a REDOR filtering element which spans six rotor periods and which dephases magnetization of nitrogen-bonded protons (Fig. 5a). Magnetization of other protons is essentially preserved due to the

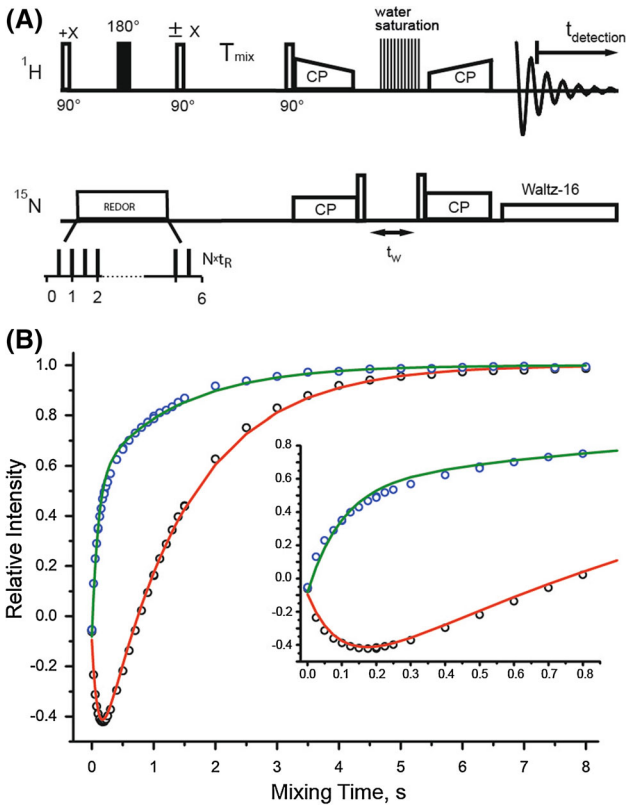

Fig. 5 **a** NMR pulse scheme to measure spin diffusion between H^N protons and the pool of residual ^1H magnetization. Amide magnetization is initially suppressed using a REDOR filter element, while proton magnetization of non-nitrogen-bonded protons is essentially preserved. A variable spin diffusion mixing time T_{mix} allows for magnetization transfer from water and residual protons in the protein to the amide protons which are subsequently observed during $t_{detection}$. Forty-four points were acquired for each experiment with the initial magnetization of the remaining protons being aligned either opposite or along the direction of the Boltzmann equilibrium magnetization. **b** Magnetization build-up curves of the H^N bulk magnetization as a function of the ^1H,^1H spin diffusion time, obtained by employing the pulse sequence shown in Fig. 4a. *Green* and *black circles* represent experiments for which the remaining ^1H magnetization was aligned either along or opposite to the Boltzmann equilibrium magnetization prior to the mixing period. *Continuous lines* show the numerically obtained fit of the experimental data. The *inset* shows the evolution of magnetization for short mixing times

low proton content in deuterated samples, which results in long transverse magnetization lifetimes. After the dipolar dephasing period, the proton 90° pulse returns proton magnetization along or opposite to the Z-axis. During the subsequent mixing period T_{mix} (spin diffusion), magnetization is transferred from H_2O and hydroxyl protons of the protein to the amide protons, which are then detected in 1D mode. For both initial alignments of the magnetization remaining proton polarization, we recorded 44 points employing different mixing times. The CP contact time was set to 410 μs to allow only for transfer between directly bonded proton and nitrogen nuclei. The delay t_w

for suppression of the water artifact was set to ca. 8 ms. The RF field strength of the applied pulses was the same as in the HETCOR experiments described above.

During the mixing period, a complex spin dynamics take place, which was fitted in the framework of a simplified model.

For quantification, we consider an amide proton interacting with N_W absolutely equivalent water protons, which can be described by a system of two differential equations:

$$\frac{\mathrm{d}}{\mathrm{d}t}\begin{pmatrix} M_{\mathrm{HN},z}(t) \\ M_{W,z}(t) \end{pmatrix} = \begin{pmatrix} -R_{\mathrm{HN},1} - k & k \\ k/N_{\mathrm{W}} & -R_{W,1} - k/N_{\mathrm{W}} \end{pmatrix} \begin{pmatrix} \Delta M_{\mathrm{HN},z}(t) \\ \Delta M_{\mathrm{W},z}(t) \end{pmatrix} \quad (2)$$

The average longitudinal magnetization of a single ^{1}H spin in water and of an amide proton spin is denoted as $M_{W,z}$ and $M_{HN,z}$. The associated longitudinal relaxation rates are referred as $R_{W,1}$ and $R_{HN,1}$, respectively. The difference between the actual magnetization and its thermal equilibrium value is denoted as $\Delta M_{HM,z}$ and $\Delta M_{W,z}$ for amide and water protons, respectively. The polarization exchange rate between amide and water proton is abbreviated as k. Least squares fitting was performed in MATLAB using an in-build optimization routine. We assumed that the REDOR filter does not perform perfectly, which requires use of additional fitting parameters like nonzero initial amide magnetization and partial suppression of non-^{15}N bound protons. The water magnetization $M_{W,z}$ ($t = 0$) after the recycle delay d_1 was given as

$$M_{W,z}(t=0) = M_{W,z}(t=\infty) \cdot \left[1 - e^{-\mathrm{d}_1 \cdot R_{W,1}}\right] \quad (3)$$

where the water magnetization at Boltzmann equilibrium is given by $M_{W,z}$ ($t = \infty$) and calculated during the fit.

Assuming that a single amide proton interacts with 20 water molecules, as discussed by Böckmann et al. (Boeckmann et al. 2009), we find $R_{HN,1} = 0.0$ s^{-1}, $R_{W,1} = 0.84$ s^{-1} and $k = 8.8$ s^{-1} for the combined two experimental data sets. This shows that due to fast magnetization exchange with the substantial water pool, the longitudinal evolution of H^N magnetization is determined mostly by the longitudinal dynamics of the water polarization and the exchange rate k. At the same time, the experimental recovery time of the longitudinal magnetization of the amide protons amounts to 1.5 s which is close to $1/R_{W,1} = 1.19$ s. This is in agreement with the conclusion that the recovery time for amide longitudinal magnetization is close to the water relaxation rate due to the very high magnetization exchange rate between water and amides. The value $R_{HN,1} = 0.0$ is not reliably determined by the fitting procedure, and it is physically meaningless. Using fixed values for $R_{HN,1}$ in the range of 0 and 1 s^{-1} during the fit we obtain only small variations of the other fitted parameters (within 8 %). These show that $R_{HN,1}$ does not have strong coupling to other parameters and can not be captured with good accuracy.

The obtained exchange rate $k = 8.8$ s^{-1} corresponds to a dipolar coupling between two protons which are 25 Å apart. Even in a strongly deuterated sample, a sphere of this radius contains a lot more than 20 H_2O molecules. We performed additional data fitting considering a different numbers of water protons which interact with an individual amide proton. The data are given in the Table S1 of the Supporting Information and show similar results for $R_{W,1}$ and k when the number of water protons varies from three to an infinite amount. The stability of the fitting approach indicates that the obtained values describe the magnetization transfer in the system at first approximation physically correct.

Conclusion

We have shown that solvent and residual protein polarization can be efficiently recycled in proton-detected MAS solid-state NMR experiments applied to highly deuterated proteins. The approach yields a sensitivity enhancement factor of 1.3 in a 1D version of the HCOCACONH experiment. The corresponding 3D experiment suffers from water artifact and would require pulsed field gradients to benefit to full extend from the flip-back approach. In case of efficient water suppression, the experimental time could be reduced by a factor of 1.7. The sensitivity in the 2D HN correlation experiment can be enhanced by a factor 1.1. We quantitatively described longitudinal magnetization exchange between amide protons and water which determines the observable sensitivity enhancement.

Acknowledgments We thank Brigitta Angerstein for expert technical assistance. This work was supported by the Max Planck Society, the Leibniz-Gemeinschaft, and the DFG (Emmy Noether Fellowship to A.L). A.L. and S.X. acknowledge funding from the CRC803 (DFG).

References

Akbey U et al (2010) Optimum levels of exchangeable protons in perdeuterated proteins for proton detection in MAS solid-state NMR spectroscopy. J Biomol NMR 46:67–73

Atreya HS, Szyperski T (2004) G-matrix Fourier transform NMR spectroscopy for complete protein resonance assignment. Proc Natl Acad Sci USA 101:9642–9647

Baldus M, Petkova AT, Herzfeld J, Griffin RG (1998) Cross polarization in the tilted frame: assignment and spectral simplification in heteronuclear spin systems. Mol Phys 95:1197–1207

Bennett AE, Rienstra CM, Griffiths JM, Zhen WG, Lansbury PT, Griffin RG (1998) Homonuclear radio frequency-driven recoupling in rotating solids. J Chem Phys 108:9463–9479

Boeckmann A et al (2009) Characterization of different water pools in solid-state NMR protein samples. J Biomol NMR 45:319–327

Chevelkov V et al (2003) H-1 detection in MAS solid-state NMR Spectroscopy of biomacromolecules employing pulsed field gradients for residual solvent suppression. J Am Chem Soc 125:7788–7789

Chevelkov V, Faelber K, Diehl A, Heinemann U, Oschkinat H, Reif B (2005) Detection of water molecules in a polycrystalline sample of a chicken a-spectrin SH3 domain. J Biomol NMR 31:295–310

Chevelkov V, Rehbein K, Diehl A, Reif B (2006) Ultrahigh resolution in proton solid-state NMR spectroscopy at high levels of deuteration. Angew Chem Int Ed 45:3878–3881

Chevelkov V, Fink U, Reif B (2009) Quantitative analysis of backbone motion in proteins using MAS solid-state NMR spectroscopy. J Biomol NMR 45:197–206

Chevelkov V, Giller K, Becker S, Lange A (2013) Efficient CO-CA transfer in highly deuterated proteins by band-selective homonuclear cross-polarization. J Magn Reson 230:205–211

Chevelkov V, Habenstein B, Loquet A, Giller K, Becker S, Lange A (2014) Proton-detected MAS NMR experiments based on dipolar transfers for backbone assignment of highly deuterated proteins. J Magn Reson 242:180–188

Delaglio F, Grzesiek S, Vuister GW, Zhu G, Pfeifer J, Bax A (1995) NMRPIPE—a multidimensional spectral processing system based on UNIX pipes. J Biomol NMR 6:277–293

Emsley L, Bodenhausen G (1990) Gaussian pulse cascades—new analytical functions for rectangular selective inversion and in-phase excitation in NMR. Chem Phys Lett 165:469–476

Ernst RR, Bodenhausen G, Wokaun A (1987) Principles of nuclear magnetic resonance in one and two dimensions. Clarendon, Oxford

Ganapathy S, Naito A, McDowell CA (1981) Paramagnetic doping as an aid in obtaining high-resolution C-13 NMR-spectra of biomolecules in the solid-state. J Am Chem Soc 103:6011–6015

Giffard M, Bardet M, Bersch B, Coves J, Hediger S (2009) Impact of selective excitation on carbon longitudinal relaxation: towards fast solid-state NMR techniques. J Magn Reson 200:153–160

Grzesiek S, Bax A (1993) The importance of not saturating H2O in protein nmr—application to sensitivity enhancement and NOE measurements. J Am Chem Soc 115:12593–12594

Helmus JJ, Surewicz K, Nadaud PS, Surewicz WK, Jaroniec CP (2008) Molecular conformation and dynamics of the Y145Stop variant of human prion protein. Proc Natl Acad Sci USA 105:6284–6289

Huber M, Hiller S, Schanda P, Ernst M, Bockmann A, Verel R, Meier BH (2011) A proton-detected 4D solid-state NMR experiment for protein structure determination. ChemPhysChem 12:915–918

Knight MJ et al (2011) Fast resonance assignment and fold determination of human superoxide dismutase by high-resolution proton-detected solid-state MAS NMR spectroscopy. Angew Chem Int Ed 50:11697–11701

Linser R, Chevelkov V, Diehl A, Reif B (2007) Sensitivity enhancement using paramagnetic relaxation in MAS solid-state NMR of perdeuterated proteins. J Magn Reson 189:209–216

Linser R, Bardiaux B, Higman V, Fink U, Reif B (2011) Structure calculation from unambiguous long-range amide and methyl (1)H-(1)H distance restraints for a microcrystalline protein with MAS solid-state NMR spectroscopy. J Am Chem Soc 133:5905–5912

Lopez JJ, Kaiser C, Asami S, Glaubitz C (2009) Higher sensitivity through selective (13)C excitation in solid-state NMR spectroscopy. J Am Chem Soc 131:15970–15971

Loquet A, Lv G, Giller K, Becker S, Lange A (2011) C-13 spin dilution for simplified and complete solid-state NMR resonance assignment of insoluble biological assemblies. J Am Chem Soc 133:4722–4725

Loquet A et al (2012) Atomic model of the type III secretion system needle. Nature 486:276–279

Lupulescu A, Frydman L (2011) Sensitizing solid state nuclear magnetic resonance of dilute nuclei by spin-diffusion assisted polarization transfers. J Chem Phys 135:134202. doi:10.1063/1.3643116

Mori S, Abeygunawardana C, Johnson MO, Vanzijl PCM (1995) Improved sensitivity of HSQC spectra of exchanging protons at short interscan delays using a new fast HSQC (FHSQC) detection scheme that avoids water saturation. J Magn Reson Ser B 108:94–98

Nadaud PS, Helmus JJ, Sengupta I, Jaroniec CP (2010) Rapid acquisition of multidimensional solid-state NMR spectra of proteins facilitated by covalently bound paramagnetic tags. J Am Chem Soc 132:9561–9563

Nielsen NC, Bildsoe H, Jakobsen HJ, Levitt MH (1994) Double-quantum homonuclear rotary resonance: efficient dipolar recovery in magic-angle spinning nuclear magnetic resonance. J Chem Phys 101:1805–1812

Orekhov VY, Ibraghimov I, Billeter M (2003) Optimizing resolution in multidimensional NMR by three-way decomposition. J Biomol NMR 27:165–173

Paulson EK, Morcombe CR, Gaponenko V, Dancheck B, Byrd RA, Zilm KW (2003) Sensitive high resolution inverse detection NMR spectroscopy of proteins in the solid state. J Am Chem Soc 125:15831–15836

Pervushin K, Vogeli B, Eletsky A (2002) Longitudinal H-1 relaxation optimization in TROSY NMR spectroscopy. J Am Chem Soc 124:12898–12902

Pines A, Waugh JS, Gibby MG (1972) Proton-enhanced nuclear induction spectroscopy—method for high-resolution NMR of dilute spins in solids. J Chem Phys 56:1776

Saito K, Martineau C, Fink G, Taulelle F (2011) Flip-back, an old trick to face highly contrasted relaxation times: application in the characterization of pharmaceutical mixtures by CPMAS NMR. Solid State Nucl Magn Reson 40:66–71

Schanda P, Brutscher B (2005) Very fast two-dimensional NMR spectroscopy for real-time investigation of dynamic events in proteins on the time scale of seconds. J Am Chem Soc 127:8014–8015

Schanda P, Meier BH, Ernst M (2010) Quantitative analysis of protein backbone dynamics in microcrystalline ubiquitin by solid-state NMR spectroscopy. J Am Chem Soc 132:15957–15967

Shaka AJ, Keeler J, Frenkiel T, Freeman R (1983) An improved sequence for broad-band decoupling—WALTZ-16. J Magn Reson 52:335–338

Stonehouse J, Shaw GL, Keeler J, Laue ED (1994) Minimizing sensitivity losses in gradient-selected N-15-H-1 hsqc spectra of proteins. J Magn Reson Ser A 107:178–184

Tegenfeldt J, Haeberlen U (1979) Cross polarization in solids with flip-back of I-spin magnetization. J Magn Reson 36:453–457

Verel R, Ernst M, Meier BH (2001) Adiabatic dipolar recoupling in solid-state NMR: the DREAM scheme. J Magn Reson 150:81–99

Vranken WF et al (2005) The CCPN data model for NMR spectroscopy: development of a software pipeline. Proteins 59:687–696

Wasmer C, Lange A, Van Melckebeke H, Siemer AB, Riek R, Meier BH (2008) Amyloid fibrils of the HET-s(218-289) prion form a beta solenoid with a triangular hydrophobic core. Science 319:1523–1526

Wickramasinghe NP et al (2009) Nanomole-scale protein solid-state NMR by breaking intrinsic H-1 T-1 boundaries. Nat Methods 6:215–218

Yamamoto K, Xu JD, Kawulka KE, Vederas JC, Ramamoorthy A (2010) Use of a copper-chelated lipid speeds up NMR measurements from membrane proteins. J Am Chem Soc 132:6929–6931

Zhou DH, Rienstra CM (2008) High-performance solvent suppression for proton detected solid-state NMR. J Magn Reson 192:167–172

Zhou DH, Shah G, Cormos M, Mullen C, Sandoz D, Rienstra CM (2007a) Proton-detected solid-state NMR Spectroscopy of fully protonated proteins at 40 kHz magic-angle spinning. J Am Chem Soc 129:11791–11801

Zhou DH et al (2007b) Solid-rate protein-structure determination with proton-detected triple-resonance 3D magic-angle-spinning NMR spectroscopy. Angew Chem Int Ed 46:8380–8383